J|A|C|S
ARTICLES
Published on Web 03/28/2002

Sol−Gel Encapsulated Horseradish Peroxidase: A Catalytic Material for Peroxidation

Kevyn Smith,[†] Nathan J. Silvernail,[†] Kenton R. Rodgers,*[,†] Timothy E. Elgren,*[,‡] Mauro Castro,[‡] and Robert M. Parker[‡]

Contribution from the Department of Chemistry, North Dakota State University, Fargo, North Dakota 58105, and Department of Chemistry, Hamilton College, Clinton, New York, 13323

Received September 21, 2001. Revised Manuscript Received January 9, 2002

Abstract: This study addresses the viability of sol−gel encapsulated HRP (HRP:sol−gel) as a recyclable solid-state catalytic material. Ferric, ferric-CN, ferrous, and ferrous-CO forms of HRP:sol−gel were investigated by resonance Raman and UV−visible methods. Electronic and vibrational spectroscopic changes associated with changes in spin state, oxidation state, and ligation of the heme in HRP:sol−gel were shown to correlate with those of HRP in solution, showing that the heme remains a viable ligand-binding complex. Furthermore, the high-valent HRP:sol−gel intermediates, compound I and compound II, were generated and identified by time-resolved UV−visible spectroscopy. Catalytic activity of the HRP:sol−gel material was demonstrated by enzymatic assays by using I^-, guaiacol, and ABTS as substrates. Encapsulated HRP was shown to be homogeneously distributed throughout the sol−gel host. Differences in turnover rates between guaiacol and I^- implicate mass transport of substrate through the silicate matrix as a defining parameter in the peroxidase activity of HRP:sol−gel. HRP:sol−gel was reused as a peroxidation catalyst for multiple reaction cycles without loss of activity, indicating that such materials show promise as reusable catalytic materials.

Introduction

In recent years, enzymes and proteins encapsulated in sol−gel derived silica glasses have been extensively studied.[1−4] Upon encapsulation, many enzymes and proteins retain their native functions and spectroscopic properties.[5] The resulting bio-composite materials are permeable to a wide variety of molecules, but retain the entrapped biomolecule.[6] Much current research is aimed at exploiting the high reactivity and specificity of enzymes and proteins for chemical and biochemical sensing.[1,7] In addition to sensing, these bio-composite sol−gels could serve as recyclable catalytic materials for laboratory or industrial scale reactions. Solid-state enzyme:sol−gel materials would have the enzyme protected from thermal and/or microbial degradation and would facilitate catalyst recovery by centrifugation or filtration. However, such materials would only be useful (a) if the necessary catalytic intermediates were accessible, (b) if mass transport of substrates and products to and from the enzyme active site through the sol−gel matrix were not severely rate limiting, and (c) if the catalyst could be recovered and recycled without losing a significant amount of activity. This report presents evidence that all of these criteria can be met by using sol−gel encapsulated horseradish peroxidase (HRP:sol−gel).

Sol−gel synthesis involves hydrolysis of siloxanes ($Si(OR)_4$), which leads to condensations and polymerizations that ultimately yield the solid sol−gels. Initial hydrolysis affords low molecular weight μ-oxo-bridged siloxane oligomers. As condensation continues, cross-linking between oligomers increases the viscosity of the sol, eventually forming a solid porous material.[8] Sonication of the sol during the initial hydrolysis and condensation reactions eliminates the need for often used cosolvents such as alcohols, which can promote protein denaturation. This adaptation of the sol−gel process allows for the incorporation of fragile biomolecules into the sol−gel matrix.[9]

Much of the research effort on bio-composite sol−gels has focused on optical sensing wherein signals are derived from colorimetric reactions involving an analyte and the encapsulated

* To whom correspondence should be addressed. E-mail: Kent_Rodgers@ndsu.nodak.edu.
[†] North Dakota State University.
[‡] Hamilton College.

(1) Dave, B. C.; Dunn, B.; Valentine, J. S.; Zink, J. I. *Anal. Chem.* **1994**, *66*, 1120A.
(2) Dunn, B.; Miller, J. M.; Dave, B. C.; Valentine, J. S.; Zink, J. I. *Acta Mater.* **1998**, *46*, 737.
(3) Dave, B. C.; Miller, J. M.; Dunn, B.; Valentine, J. S.; Zink, J. I. *J. Sci. Technol.* **1997**, *8*, 629.
(4) Armon, R.; Dosoretz, C.; Starosvetsky, J.; Orshansky, R.; Saadi, I. *J. Biotechnol.* **1996**, *51*, 279.
(5) (a) Guilbault, G. G. *Analytical Uses of Immobilized Enzymes*; Marcel Dekker: New York, 1984. (b) Gill, I.; Ballesteros, A. *Trends Biotechnol.* **2000**, *18*, 282−296.
(6) Lan, E. H.; Dave, B. C.; Fukuto, J. M.; Dunn, B.; Zink, J. I.; Valentine, J. S. *J. Mater. Chem.* **1999**, *9*, 45.
(7) Blyth, D. J.; Aylott, J. W.; Richardson, D. J.; Russell, D. A. *Analyst* **1995**, *120*, 2725.
(8) Brinker, C. J.; Scherer, G. W. *Sol−Gel Science*; Academic Press: San Diego, 1990; pp 97−235.
(9) Ellerby, L. M.; Nishida, C. R.; Nishida, F.; Yamanaka, S. A.; Dunn, B.; Valentine, J. S.; Zink, J. I. *Science.* **1992**, *255*, 1113.

enzyme or protein. Examples include myoglobin,[1,6,7,10] hemoglobin,[1,6,7,11−13] cytochrome *c*,[2,3,6,9,14] glucose oxidase,[1,15−17] alkaline phosphatase,[18] Cu−Zn superoxide dimutase,[1,9] urease,[20,21] trypsin,[22] bacteriorhodopsin,[1,19,23] horseradish peroxidase,[24−27] lactoperoxidase,[28] nitrate reductase,[29] atrazine chlorohydrolase,[30] and photoprotein.[31] All have been shown to retain most or all of their biological function and activity while encapsulated in a sol−gel matrix. Optical sensors based on bio-composite sol−gels have proven effective for the detection of hydrogen peroxide,[25,26] glucose,[32−35] nitrate,[29] nitric oxide,[6,7,9] carbon monoxide,[7,9,12,13] oxygen,[1,9,10] phenols,[27] oxalate,[1] and aqueous Fe^{III}.[36] Although the potential of bio-composite sol−gels as recyclable catalytic materials has been explored,[5b] this application seems to have received less attention than sensors. The present study investigates the viability of encapsulated horseradish peroxidase (HRP:sol−gel) as a catalytic material for peroxidation.

HRP (oxidoreductase, EC 1.11.1.7) is an extensively characterized peroxidase that catalyzes the oxidation of various molecules by H_2O_2 (see Scheme 1). The active site of HRP contains a protoheme that is bound to the enzyme through axial coordination by the imidazole side chain of a proximal histidine residue.[37] The catalytic cycle of HRP involves stepwise two-electron oxidation of the ferric heme by H_2O_2, generating an oxo ferryl protophyrin IX π-cation radical, compound I (HRP-I).[38−40] Compound II (HRP-II), the second intermediate in the HRP catalytic cycle, is formed by one-electron reduction of

Scheme 1

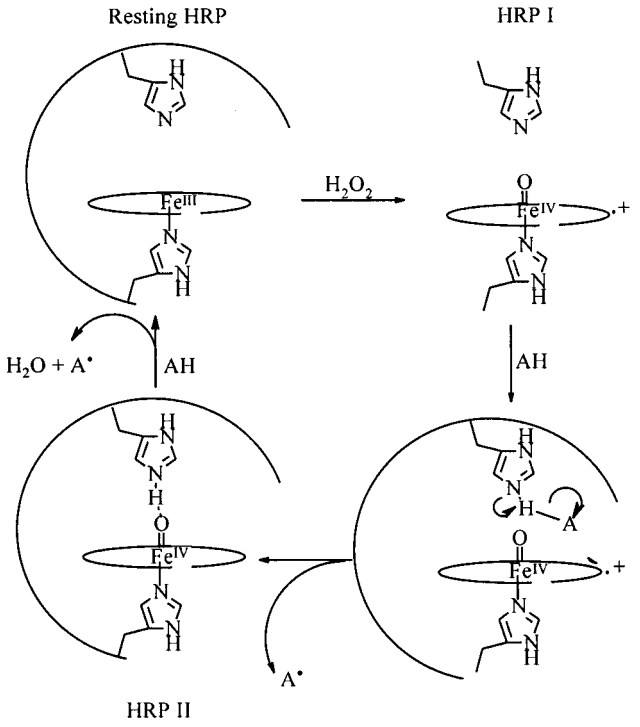

HRP-I where the Fe^{IV}═O center is maintained and the porphyrin π cation radical is reduced.[41,42] Numerous spectroscopic studies of HRP including resonance Raman (rR),[43−47] UV−vis, electron paramagnetic resonance (EPR),[48−50] NMR,[49] and IR[51,52] investigations have been reported. Because HRP is well understood from both structural and mechanistic standpoints, and because the correlations between spectral signatures and states of the enzyme are well established,[53−56] it presents an excellent paradigm for testing bio-composite sol−gels as recyclable catalytic materials. Herein, we report spectroscopic and enzyme activity data that reveal similarities in the heme environments and reactivities of aqueous HRP and HRP:sol−gel. These similarities have been demonstrated with rR and UV−visible spectroscopic methods, which provide insight into heme spin state, oxidation state, and coordination number. The minimal influence of sol−gel encapsulation on heme structure and reactivity is inferred from comparison of spectroscopic parameters and catalytic activities between the encapsulated and solution forms of HRP. Furthermore, peroxidase activities measured in successive reaction cycles provide the first evidence

(10) Chung, K. E.; Lan, E. H.; Davidson, M. S.; Dunn, B.; Valentine, J. S.; Zink, J. I. *Anal. Chem.* **1995**, *67*, 1505.
(11) Shibayama, N.; Saigo, S. *J. Mol. Biol.* **1995**, *251*, 203.
(12) Juszczak, L. J.; Friedman, J. M. *J. Biol. Chem.* **1999**, *274*, 30357.
(13) Shibayama, N.; Saigo, S. *J. Am. Chem. Soc.* **1999**, *121*, 444.
(14) Miller, J. M.; Dunn, B.; Valentine, J. S.; Zink, J. I. *J. Noncryst. Solids*. **1996**, *202*, 279.
(15) Yamanaka, S. A.; Nishida, F.; Ellerby, L. M.; Nishida, C. R.; Dunn, B.; Selverstone, V. J.; Zink, J. I. *Chem. Mater*. **1992**, *4*, 495.
(16) Shtelzer, S.; Braun, S. *Biotechnol. Appl. Biochem*. **1994**, *19*, 293.
(17) Narang, U.; Prasad, P. N.; Bright, F. V.; Ramanathan, K.; Deepak-Kumar, N.; Malhorta, B. D.; Kamalasanan, M. N.; Chandra, S. *Anal. Chem*. **1994**, *66*, 3139.
(18) Braun, S.; Rappoport, S.; Zusman, R.; Avnir, D.; Ottolenghi, M. *Mater. Lett.* **1990**, *10*, 1.
(19) Avnir, D.; Braun, S.; Lev, O.; Ottolenghi, M. *Chem. Mater*. **1994**, *6*, 1605.
(20) Kurokawa, Y.; Sano, T.; Ohta, H.; Nakagawa, Y. *Biotechnol. Bioeng.* **1993**, *42*, 394.
(21) Narang, U.; Prasad, P.; Bright, F. V. *Chem. Mater*. **1994**, *6*, 1596.
(22) Avnir, D.; Braun, S.; Ottolenghi, M. *Supramolecular Architecture in Two and Three Dimensions*; Bein, T., Ed.; American Chemical Society: Washington, DC, 1992; Vol. 499, p 384.
(23) Wu, S.; Ellerby, L. M.; Cohan, J. S.; Dunn, B.; El-Sayed, M. A.; Selverstone, V. J.; Zink, J. I. *Chem. Mater*. **1993**, *5*, 1605.
(24) Wu, S.; Lin, J.; Chan, S. I. *Appl. Biochem. Biotechnol*. **1994**, *47*, 11.
(25) Navas Diaz, A.; Ramos Peinado, M. C.; Torijas Minguez, M. C. *Anal. Chim. Acta* **1998**, *363*, 221.
(26) Chut, S. L.; Li, J.; Tan, S. N. *Analyst* **1997**, *122*, 1431.
(27) Kane, S. A.; Iwuoha, E. I.; Smyth, M. R. *Analyst* **1998**, *123*, 2001.
(28) Smith, J. K.; Rodgers, K. R. Unpublished results.
(29) Aylott, J. W.; Richardson, D. J.; Russell, D. A. *Analyst* **1997**, *122*, 77.
(30) Kauffmann, C.; Mandelbaum, R. T. *J. Biotechnol.* **1998**, *62*, 169.
(31) Blyth, D. J.; Poynter, S. J.; Russell, D. A. *Analyst* **1996**, *121*, 1975.
(32) Yang, S.; Lu, Y.; Atanossov, P.; Wilkins, E.; Long, X. *Talanta* **1998**, *47*, 735.
(33) Tatsu, Y.; Tamashita, K.; Yamaguchi, M.; Yamamura, S.; Yamamoto, H.; Yoshikawa, S., *Chem. Lett.* **1992**, 1615.
(34) Gleezer, V.; Lev, O. *J. Am. Chem. Soc.* **1993**, *115*, 2533.
(35) Narang, D.; Prasad, P. N.; Bright, F. V.; Ramanathan, S.; Kumar, N. D.; Malhorta, B. D.; Kamalasanan, M. N.; Chandra, S. *Anal. Chem.* **1994**, *66*, 3139.
(36) Barrero, J. M.; Camara, C.; Perez-Conde, M. C.; San Jose, C.; Ferandez, L. *Analyst* **1995**, *120*, 431.
(37) Yonetani, T.; Yamamoto, H. *Oxidase and Related Redox Systems*; King, T. E., Mason, H. S., Morrison, M., Eds.; University Park Press: Baltimore, MD, 1973; Vol. 1, pp 279−298.
(38) La Mar, G. N.; de Ropp, J. S. *J. Am. Chem. Soc.* **1980**, *102*, 395.
(39) Schulz, C. E.; Devaney, P. W.; Winkler, H.; Debrunner, P. G.; Doan, N.; Chiang, R.; Rutter, R.; Hager, L. P. *FEBS Lett.* **1979**, *103*, 102.
(40) Rutter, R.; Hager, L. P. *J. Biol. Chem.* **1982**, *257*, 7958.
(41) Dunford, H. B. *Adv. Inorg. Biochem.* **1982**, *4*, 41−68.
(42) Frew, J. E.; Jones, P. *Adv. Inorg. Bioinorg. Mech.* **1984**, *3*, 175.
(43) Teroaka, J.; Ogura, T.; Kitagawa, T. *J. Am. Chem. Soc.* **1982**, *104*, 7354.
(44) Ogura, T.; Kitagawa, T. *J. Am. Chem. Soc.* **1987**, *109*, 2177.
(45) Oertling, W. A.; Babcock, G. T. *J. Am. Chem. Soc.* **1985**, *107*, 6406.
(46) Oertling, W. A.; Babcock, G. T. *Biochemistry* **1988**, *27*, 3331.
(47) Paeng, K. J.; Kincaid, J. R. *J. Am. Chem. Soc.* **1988**, *110*, 7913.
(48) Rutter, R.; Valentine, M.; Hendrich, M. P.; Hager, L. P.; Debrunner, P. G. *Biochemistry* **1983**, *22*, 4769.
(49) Leigh, J. S.; Maltempo, M. M.; Ohlsson, P. I.; Paul, K. G. *FEBS Lett.* **1975**, *51*, 304.
(50) Aasa, R.; Vanngard, T.; Dunford, B. H. *Biochim. Biophys. Acta* **1975**, *391*, 259.
(51) Barlow, C. H.; Ohlsson, P.-I.; Paul, K. G. *Biochemistry* **1976**, *15*, 2225.
(52) Smith, M. L.; Ohlsson, P.-I.; Paul, K. G. *FEBS Lett.* **1983**, *163*, 303.
(53) Palaniappan, V.; Terner, J. *J. Biol. Chem.* **1989**, *264*, 16046.
(54) Kitagawa, T. *Pure Appl. Chem*. **1987**, *59*, 1285.
(55) Feis, A.; Marzocchi, M. P.; Paoli, M.; Smulevich, G. *Biochemistry* **1994**, *33*, 4577.
(56) Desbois, A.; Mazza, G.; Stetzkowski, F.; Lutz, M. *Biochim. Biophys. Acta* **1984**, *785*, 161.

that bio-composite sol−gels could find use as recyclable catalytic materials.

Experimental Section

Materials. Lyophilized HRP (isoenzyme C) was purchased from Sigma and used without further purification. Silica sol was prepared with tetramethyl orthosilicate (TMOS) or tetraethyl orthosilicate (TEOS) as precursors. The TMOS sol consisted of 1.5 mL of TMOS, 0.35 mL of Nanopure water, and 0.01 mL of 0.1 M HCl, which was sonicated for 30 min prior to protein incorporation.[9] TMOS-derived HRP:sol−gels were produced by addition of the sol to 50 μM HRP dissolved in 10 mM phosphate at pH 6.8. The TEOS sol contained 4.5 mL of TEOS, 1.4 mL of Nanopure water, and 0.100 mL of 0.1 M aqueous HCl. This mixture was allowed to sit for 1 h in an ultrasonic cleaning bath at ambient temperature, after which it was stored at −20 °C for 10 days.[57] TEOS-derived gels were produced by mixing 0.390 mL of 51 μM HRP (in 20 mM phosphate buffer, 100 mM NaCl, 10% glycerol, pH 6.8) with 0.240 mL of the sol.

Casting of Sol−Gel Monoliths. TMOS-derived monoliths were prepared by mixing 0.240 mL of the sol with 0.390 mL of 50 μM HRP. This mixture was then placed on the optical side of a glass cuvette creating a film (approximately 2 mm thick) with the length and width being defined by the cuvette. Monoliths were solid within 30 min. They were rinsed three times with 3-mL aliquots of 10 mM sodium phosphate buffer, pH 6.8, and stored in the buffer for 24 h at room temperature. For two weeks following gelation, the monoliths were rinsed daily with 10 mM sodium phosphate buffer, pH 6.8, and stored until the next wash in phosphate buffer at room temperature.

The TEOS-derived monoliths were prepared by pouring the aforementioned mixuture of sol and enzyme solution onto an optical face of a UV−visible cuvette and allowing it to cure for 10 min. The cuvettes were then filled with 20 mM phosphate buffer, pH 6.8, 100 mM NaCl, 10% glycerol, and stored at 4 °C overnight. This buffer was replaced with at least three fresh aliquots of buffer to remove the ethanol produced in the gelation reaction.

Preparation of HRP:Sol−Gel Pellets and Powders. Gels aged for two weeks in phosphate buffer were carefully dried for 3 days at room temperature. The resulting xerogels were broken into small pellets. Powders were generated by grinding the dried sol−gel pellets in an agate mortar and pestle.

Casting of Thin Films in NMR Tubes. Thin films were generated by mixing 0.040 mL of sol and 0.060 mL of 50 μM HRP. Immediately after mixing, sol solutions were transferred to an NMR tube that was spun at ∼70 Hz for 30 min. Once solidified, HRP:sol−gels were treated as described above for the monoliths.

Casting of Cylindrical Sol−Gels. Cyclindrical sol−gels were cast in glass tubes from TMOS sols prepared as described above. The sol−gels produced by this method were removed from the glass tubes by extrusion.

Reactions of HRP:Sol−Gel. HRP:sol−gel samples were used between ages three and eight weeks. HRP−CN:sol−gel was generated by placing 0.2 mL of 10 mM KCN in 10 mM sodium phosphate buffer, pH 6.8, in contact with the thin films. Reduction of HRP:sol−gel was achieved by adding 10 μL of buffered 574 μM $Na_2S_2O_4$ directly to 0.1 mL of 10 mM phosphate buffer, pH 6.8, that was already present in the NMR tube. Ferrous HRP−CO:sol−gel was generated by syringing CO at 1 atm into the NMR tube containing the thin film of ferrous HRP:sol−gel. HRP−I:sol−gel was generated in TEOS-derived HRP:sol−gel monoliths by adding a 2-fold molar excess of H_2O_2 to 20 mM sodium phosphate buffer, pH 6.8, at 17 °C.

Iodide Assays with Pellets and Powders of HRP:Sol−Gel. Peroxidase assays were carried out in a 4 mL glass cuvette equipped with a magnetic stir flea. Injection and abstraction of solutions was achieved by using two 2-mm OD Teflon tubes fixed in a rubber stopper fitted to the top of the cuvette. To a cuvette containing HRP:sol−gel as either powders, pellets, or monoliths, 3 mL aliquots of 5 mM KI in 33 mM phosphate, pH 7.0, were added and allowed to equilibrate for 2 min. Generation of I_3^- was initiated by addition of 0.3 mL of 1.5 mM H_2O_2. Absorbance was monitored for 2 min at 353 nm to determine the initial rate of I_3^- production. Sol−gel pellets were removed from the reaction solution and rinsed with three 3-mL washes of 33 mM sodium phosphate buffer, pH 7.0. Rinsed HRP:sol−gel pellets were then reexposed to 5 mM KI in 33 mM sodium phosphate buffer, pH 7.0, to restart the catalytic production of I_3^-. Powdered HRP:sol−gels were separated from the spent assay solution by centrifugation. Blank sol−gels and I^- assay solutions were exposed to the same reaction conditions described above to quantify the noncatalytic oxidation. Each initial rate measurement was corrected for noncatalytic production of I_3^-. All assays and blank runs were performed in triplicate.

Guaiacol Assays with Pellets and Powders of HRP:Sol−Gel. With use of the same conditions described above for the I^- assay, peroxidation activity was measured for guaiacol. Assay solutions contained 3 mL of 33 mM guaiacol in 100 mM sodium phosphate buffer, pH 7.4. This solution was added to an optical cuvette containing HRP:sol−gel as pellets, monoliths, or powders. Peroxidation was initiated by addition of H_2O_2 and guaiacol oxidation was tracked by the increase in optical absorbance at 470 nm ($\epsilon_{470} = M^{-1}\cdot cm^{-1}$). Equilibration studies were conducted by allowing HRP:sol−gel to equilibrate with the guaiacol solution for 30 min prior to addition of H_2O_2. Blank measurements similar to those described for the I^- assays were used to correct for noncatalytic oxidation.

Reactions Involving Cylindrical HRP:Sol−Gels. Activity assays of cylindrical HRP:sol−gel samples were accomplished by a fixed-time procedure wherein the cylinder was placed in a solution containing H_2O_2 and ABTS (2,2′-azinodi(3-ethylbenzthiazolinesulfonic acid)) and agitated for 10 min. The HRP:sol−gel was then removed and the solution was analyzed by optical absorbance at 404 nm ($\epsilon_{404} = 17200$ $M^{-1}\cdot cm^{-1}$) to quantify ABTS peroxidation.

Spectroscopy. Resonance Raman spectra were recorded by using emission from a Kr^+ (406.7 nm, 413.1 nm) or He/Cd (441.6 nm) laser. Spectra were recorded on a spectrometer comprising a 0.64 m monochromator equipped with a 2400 line/mm holographic grating and a liquid N_2 cooled CCD camera. Samples were contained in 5 mm NMR tubes and spun at approximately 30 Hz. The laser beam was focused to a line at the sample with a cylindrical lense. Scattered light was collected in the 135° backscattering geometry. Raman spectra were calibrated by using known Raman frequencies for neat indene, cyclohexane, toluene, methylene bromide, and pentane. UV−visible absorbance spectra were recorded on a commercial scanning double spectrophotometer interfaced to a PC. Wavelength calibration was verified with use of holmium oxide glass.

Results and Discussion

Comparing the Hemes of HRP:Sol−Gel and Aqueous HRP. Figure 1 shows the 406.7 nm excited resonance Raman (rR) spectra of aqueous HRP and HRP:sol−gel at room temperature. The Soret-excited rR spectra between 1300 and 1650 cm^{-1} indicate the heme of HRP:sol−gel retains spectroscopic properties similar to those reported in aqueous solution.[53,54,58,59] Precedence for this observation is found in similar experiments carried out on hemoglobin (Hb),[60] myoglobin,[61] and cytochrome *c*.[62] In its resting state, HRP contains a ferric

(57) Zheng, L.; Flora, K.; Breanan J. *Chem. Mater.* **1998**, *10*, 3974−3983.
(58) Smulevich, G.; English, A. M.; Mantini, A. R.; Marzocchi, M. P. *Biochemistry* **1991**, *30*, 772.
(59) Rakshit, G.; Spiro, T. G. *Biochemistry* **1974**, *13*, 5317.
(60) Das, T. K.; Khan, I.; Rousseau, D. L.; Friedman, J. M. *Biospectroscopy* **1999**, *5*, S64−S70.
(61) Das, T. K.; Khan, I.; Rousseau, D. L.; Friedman, J. M. *J. Am. Chem. Soc.* **1998**, *120*, 10268−10269.
(62) Shen, C. Y.; Kostic, N. M. *J. Am. Chem. Soc.* **1997**, *119*, 1304−1312.

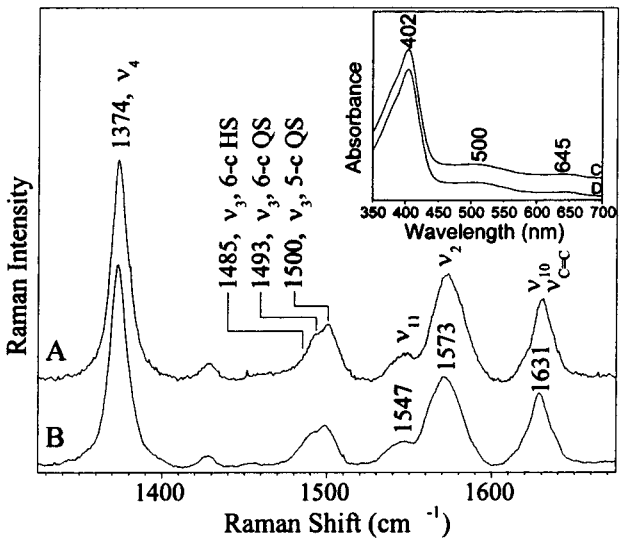

Figure 1. High-frequency rR spectra of 50 μM ferric HRP in 10 mM phosphate pH 6.8 (A) in solution and (B) in a sol−gel matrix with 406.7-nm laser excitation. The asterisk indicates a plasma line from the Kr^+ laser. Inset: Visible absorption spectra comparing solution (C) and sol−gel (D) forms of HRP. All spectra were recorded at ambient temperature.

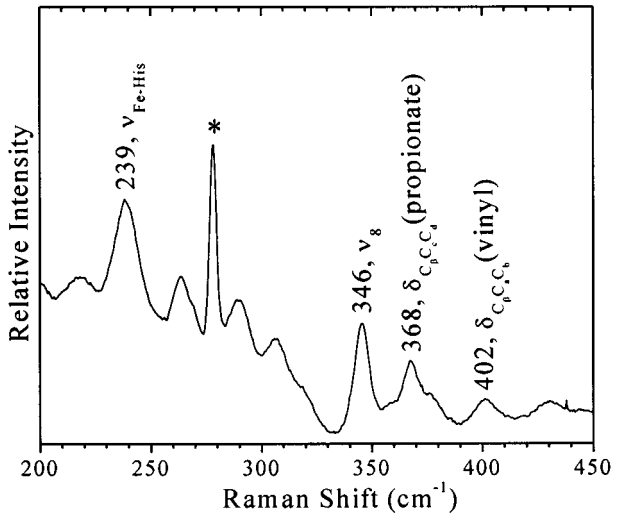

Figure 2. Low-frequency room temperature rR spectrum of ferrous HRP:sol−gel with 441.6-nm excitation. The asterisk indicates a Ne emission line from an instrument panel lamp.

protoheme linked to the protein via an Fe−His bond on the proximal side of the heme. Resting-state HRP contains an equilibrium mixture of 5-coordinate (5-c) heme and 6-coordinate (6-c) heme, which contains a water ligand bound to the distal side of the heme.[53,58,63−65] This mixture is evident from the υ_3 envelope of the rR spectra in Figure 1, which contains components at 1485 (6-c HS), 1493 (6-c QS), and 1500 cm^{-1} (5-c QS).[58,65−67] Comparison of the rR and UV−visible absorbance spectra in Figure 1 shows that speciation of the hemes in aqueous HRP and HRP:sol−gel is similar. Slight differences in the shapes of their υ_3 envelopes suggest that encapsulation within the sol−gel matrix may impact the fraction of 6-c HS heme. However, these perturbations appear to be minimal.

Heme accessibility by exogenous ligands was probed by treating HRP:sol−gel with redox reagents and small ligands. Changes in the oxidation state, axial coordination, and spin state were tracked by monitoring changes in the UV−visible and rR spectra of the heme. Changes in axial coordination and spin state are evident from the 413.1 nm excited rR spectra of HRP−CN:sol−gel. Binding of the strong-field CN^- ligand to the heme iron is indicated by shifts in the υ_3 band from 1493/1500 cm^{-1} (Figure 1) to 1507 cm^{-1} in the rR spectra (data not shown.) Complete conversion of the HS forms of HRP:sol−gel to 6-c LS HRP−CN:sol−gel shows that this small anionic ligand both permeates the sol−gel and enters the heme pocket of virtually all encapsulated HRP molecules.

It has been shown for Hb that interactions between the sol−gel matrix and the protein surface can increase the stability of the quaternary state in which the protein was encapsulated.[60] One of the well-established indicators of heme pocket conformation and conformational strain is the proximal Fe−His stretching (υ_{Fe-His}) frequency. The proximal Fe−His stretching frequencies of ferrous HRP:sol−gel and aqueous HRP were compared to probe the effect of encapsulation on this critical link between the heme and protein. Figure 2 shows that υ_{Fe-His} occurs at 239 cm^{-1} in the 441.6 nm excited rR spectrum of ferrous HRP:sol−gel. This is close to the 243 cm^{-1} Raman shift reported for aqueous HRP.[63] This frequency difference is consistent with a weakened Fe−His bond in HRP:sol−gel, which could be explained by weakened proximal His-Asp hydrogen bonding or distorting conformational forces on the proximal Fe−His bond. Although it is not clear whether this perturbation impacts the chemistry of resting ferric HRP:sol−gel, it does show that the protein can be perturbed under the influence of the encapsulating sol−gel.

The permeability of HRP:sol−gel was further probed by sequential treatment with aqueous $Na_2S_2O_4$ followed by the neutral π-acid ligand, CO.[68] Figure 3 shows the rR spectra recorded to track these transformations. Shifts in the π^* electron density marker band, υ_4, from 1374 (resting ferric) to 1358 (5-c HS ferrous) to 1372 cm^{-1} (ferrous-CO) and in the spin state marker, υ_3 , from 1485, 1493, and 1500 cm^{-1} (6-c HS, 5-c QS, and 5-c QS ferric, respectively) to 1473 cm^{-1} (5-c HS ferrous) and to 1500 cm^{-1} (6-c LS ferrous-CO) indicate sequential reduction and ligation of HRP.

Catalytic Intermediates in HRP:Sol−Gel. Essential to catalytic peroxidase activity of HRP is the generation of HRP-I upon reaction with H_2O_2. Figure 4 shows the time course of UV−visible spectral changes after treatment with a 2-fold molar excess of H_2O_2. The spectra were taken at 2 s intervals for 100 s after the addition of H_2O_2. Figure 4 shows half of the spectra recorded. Panel A shows the conversion of resting HRP:sol−gel to HRP−I:sol−gel. The isosbestic behavior and growth of the bands at 580 and 650 nm are consistent with a clean conversion between these two species.[70] Panel B shows the spectra recorded between 40 and 100 s after addition of H_2O_2. These spectra exhibit isosbestic behavior at different wave-

(63) Teraoka, J.; Kitagawa, T. *J. Biol. Chem.* **1981**, *256*, 3969.
(64) Kitagawa, T.; Hashimoto, S.; Teraoka, J.; Nakamura, S.; Yajima, H.; Toichiro, H. *Biochemistry* **1983**, *22*, 2788.
(65) Feis, A.; Howes, B. D.; Indiani, C.; Smulevich, G. *J. Ram. Spectrosc.* **1998**, 933−938.
(66) Howes, B. D.; Rodriguez-Lopez, J. N.; Smith, A. T.; Smulevich, G. *Biochemistry* **1997**, *36*, 1532−1543.
(67) Indiani, C.; Feis, A.; Howes, B. D.; Marzocchi, M. P.; Smulevich, G. *J. Am. Chem. Soc.* **2000**, *122*, 7368−7376.
(68) Yamada, H.; Yamazaki, I. *Arch. Biochem. Biophys.* **1974**, *165*, 728.
(69) Chuang, W.-J.; Van Wart, H. E. *J. Biol. Chem.* **1992**, *267*, 13293.
(70) Coulter, E. D.; Cheek, J.; Ledbetter, A. P.; Chang, C. K.; Dawson, J. H. *Biochem. Biophys. Res. Commun.* **2000**, *279*, 1011−1015.

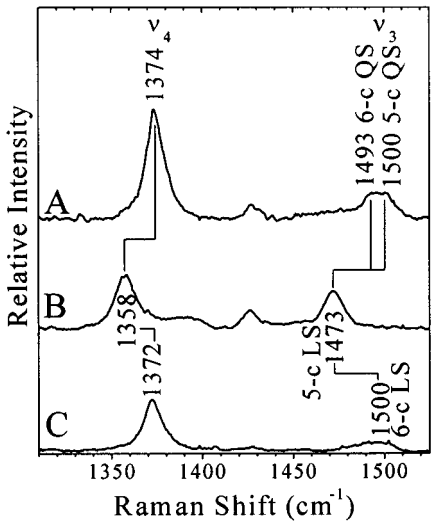

Figure 3. High-frequency rR spectra for (A) ferric HRP:sol−gel with 406.7-nm excitation, (B) ferrous HRP:sol−gel with 406.7-nm excitation, and (C) ferrous HRP−CO:sol−gel with 413.1-nm excitation. All spectra were recorded at ambient temperature.

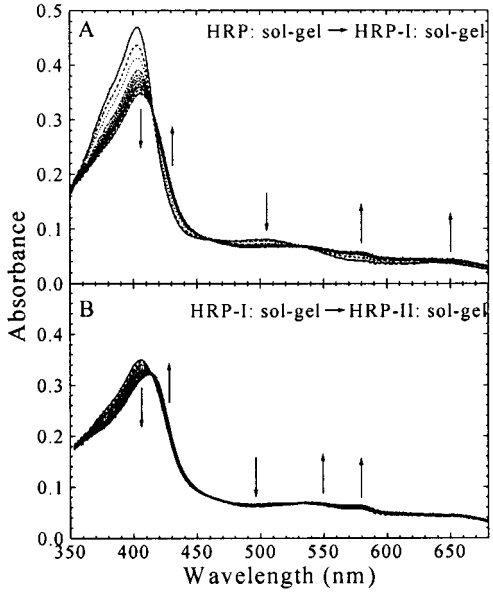

Figure 4. UV−visible spectra of HRP:sol−gel recorded after addition of a 2-fold molar excess of H_2O_2 at 17 °C. (A) Spectra recorded between 0 and 40 s after addition of H_2O_2, showing HRP:sol−gel 6 HRP−I:sol−gel conversion. (B) Spectra recorded between 40 and 100 s after addition of H_2O_2, showing HRP−I:sol−gel 6 HRP−II:sol−gel conversion.

lengths than those in panel A. Growth of the bands at 550 and 580 nm is consistent with formation of HRP−II:sol−gel.[70] This species persisted for many minutes at 17 °C. Since HRP-II is less reactive, it is more amenable to room temperature measurements.[53] Figure 5 shows the rR spectra of HRP−II:sol−gel. Shifts in υ_4 and υ_3 to 1378 and 1509 cm^{-1}, respectively, are consistent with the 6-c LS Fe^{IV}═O of HRP-II.[46,53,69]

These results show that, in addition to trapping conformational intermediates of proteins such as Hb,[60] the sol−gel matrix may support the study of other high-valent reactive intermediates relevant to important catalytic processes.

Matrix Effects on Catalytic Activity of HRP:Sol−Gel. The catalytic efficacy of encapsulated enzymes may be diminished by one or more mechanisms attributable to properties of the enzyme:sol−gel material. One of these is attenuation of substrate

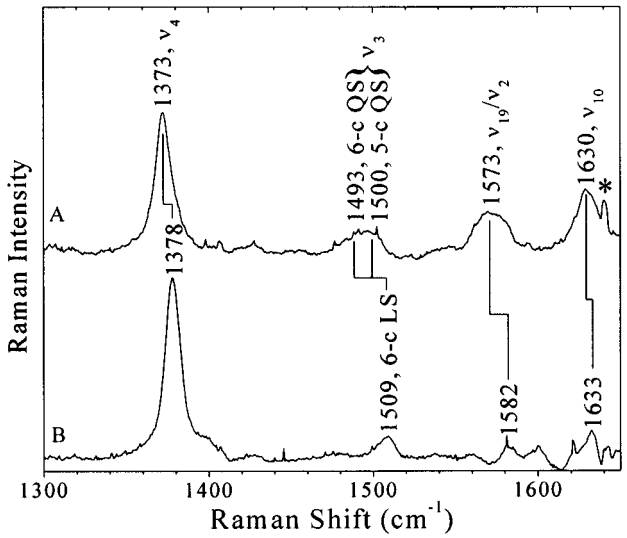

Figure 5. High-frequency 413.1-nm excited rR spectra of (A) ferric HRP:sol−gel and (B) HRP−II:sol−gel with 413.1-nm excitation. The asterisk indicates a plasma emission line from the Kr^+ laser. Both spectra were recorded at room temperature.

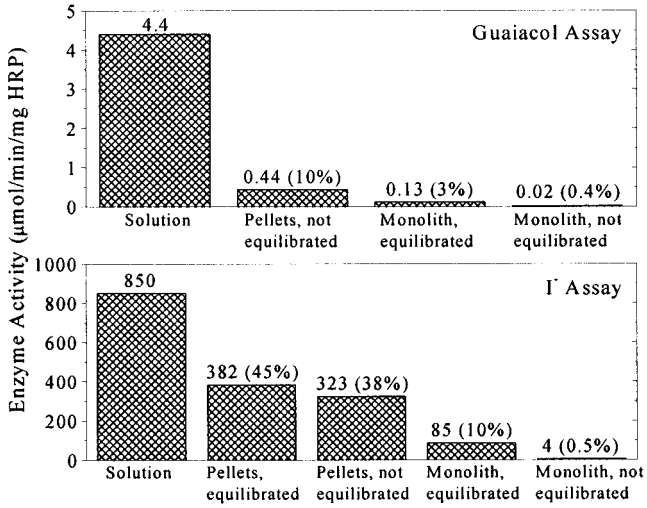

Figure 6. Comparisons of HRP:sol−gel activities with and without equilibration for guaiacol (top) and I^- (bottom) oxidation.

binding and release rates due to limitation of mass transport in to and out of the sol−gel matrix. This is likely to be a function of the sol−gel and the method of its preparation. Another is the slowing of one or more of the catalyzed reaction steps due to nonbonded interactions such as hydrogen bonding between the enzyme and its sol−gel host. This influence may depend on surface properties of both the enzyme and its sol−gel host. Correlation times of encapsulated molecules are known to increase in the sol−gel matrix. Dramatic increases in the protein correlation time have been measured for encapsulated myoglobin.[71] This suppression of molecular tumbling is clear evidence for constraining interactions between the protein and the wall of the sol−gel cavity.

With these possibilities in mind, the peroxidation activities of HRP:sol−gel pellets were compared with that of aqueous HRP. Figure 6 shows that the HRP:sol−gel activities for guaiacol and I^- peroxidation were 10% and 45% of their

(71) Gottfried, D. S.; Kagan, A.; Hoffman, B. M.; Friedman, J. M. *J. Phys. Chem. B* **1999**, *103*, 2803−2807.

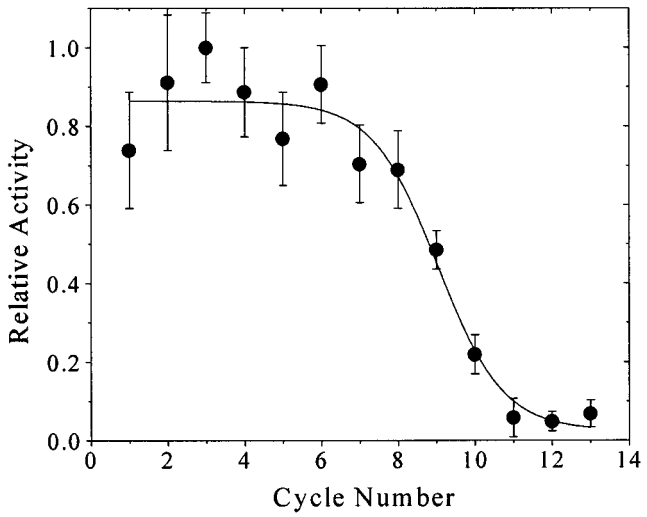

Figure 7. HRP:sol−gel activity vs cycle number. The catalyst was powdered 50 μM HRP:sol−gel, pH 7.0. The solid line is for illustrative purposes only; it does not represent a model for catalyst degradation.

solution counterparts, respectively. To address whether rate limitation by mass transport through the sol−gel matrix could account for part of the diminished activity of HRP:sol−gel, peroxidation activity was measured as a function of surface:volume ratio and equilibration time. HRP:sol−gel activities for guaiacol and I^- are summarized in Figure 6. The fractional decrease in the rate of guaiacol oxidation is substantially larger than that for I^-. Since the encapsulation environments are the same for HRP in both assays, differences in the loss of activity must be attributable to the differences between the substrates and or their oxidation products. Two of the most likely contributors to this difference are size and charge of the substrates and their oxidation products. Both of these properties are expected to impact the rate at which the substrates diffuse through the matrix to the HRP active site. Although these results suggest diminished peroxidase activity of HRP:sol−gel due to slowed mass transport, they do not represent a rigorous kinetic analysis.

The dependence of HRP:sol−gel activities upon surface:volume ratio is also apparent from Figure 6. As the surface:volume ratio was decreased from pellets to monoliths, activities for both I^- and guaiacol peroxidation decreased significantly. Because the mesh size of the pellets was not carefully controlled, it is not possible to quantify this correlation between activity and surface:volume ratio. Nevertheless, the increased activity with increased surface area suggests that the number of accessible HRP molecules increases with surface area. This correlation also indicates that the enzyme is distributed throughout the sol−gel matrix.

This distribution was further demonstrated by a series of fixed-time assays by using cylindrical samples of HRP:sol−gel. These experiments revealed a linear correlation between HRP:sol−gel activity and cylinder mass. The correlation was demonstrated by making sequential fixed-time activity assays, each after decreasing the cylinder mass by shaving with a razor blade. This demonstrates (a) that encapsulated HRP molecules are homogeneously distributed throughout the gel and (b) that HRP molecules originally in the interior of the gel are catalytically active.

The effect of recycling HRP:sol−gel on its catalytic efficacy was investigated by multiple exposures of HRP:sol−gel to the I^- assay. This series of measurements yielded the curve shown in Figure 7. HRP:sol−gel retained 38% of the aqueous HRP activity for 8 cycles. Activity declined in subsequent cycles, leveling off after 10 cycles. After many reaction cycles the heme is bleached, as judged by loss of color in the HRP:sol−gel. Hence it is likely that loss of catalytic activity is attributable to heme degradation after multiple treatments with hydrogen peroxide.

Summary

The results of this study reveal several important properties of HRP:sol−gel. First, the heme of HRP and its environment, as reported by UV−vis and rR signatures, are not significantly altered by sol−gel encapsulation. Second, neutral and charged ligands, neutral and charged redox reagents, and substrates can make their way from bulk solution to the encapsulated heme sites. Third, HRP is uniformly distributed throughout the sol−gel host. Fourth, catalytic turnover of substrates is likely rate limited, at least in part, by diffusion of substrate and/or product through the sol−gel matrix. Fourth, HRP:sol−gel retains catalytic competence through about 10 reaction cycles. Finally, HRP−I:sol−gel and HRP−II:sol−gel can be generated and observed in the absence of substrates. These observations suggest that the sol−gel matrix may be generally suited to the study of chemically reactive protein or enzyme intermediates. Given the ready availability of methods and technology to overexpress many enzymes in common, nonpathogenic organisms and the ease with which the sol−gel matrix is formed, this approach to producing laboratory and industrial catalysts may be an attractive alternative to *de novo* design and synthesis.

Acknowledgment. This work was supported by the Hermann Frasch Foundation (KRR: 446-HF97) and the Fred L. Emerson Foundation, Inc. (TEE). The authors wish to thank Prof. Gudrun Lukat-Rodgers (NDSU) and Prof. Karen S. Brewer (HC) for their insights and helpful discussions.

JA012215U